

# Lawrence Berkeley National Laboratory

## LBL Publications

### Title

Optimal design of 3D borehole seismic arrays for microearthquake monitoring in anisotropic media during stimulations in the EGS collab project

### Permalink

<https://escholarship.org/uc/item/3fh4n12f>

### Authors

Chen, Yu  
Huang, Lianjie

### Publication Date

2019-05-01

### DOI

10.1016/j.geothermics.2019.01.009

Peer reviewed

# Optimal Design of 3D Borehole Seismic Arrays for Microearthquake Monitoring in Anisotropic Media during Stimulations in the EGS Collab Project

Yu Chen, Lianjie Huang, and EGS Collab Team<sup>1</sup>

Los Alamos National Laboratory, Los Alamos, NM, 87545, USA

Corresponding authors: Yu Chen ([chenyu@lanl.gov](mailto:chenyu@lanl.gov)); Lianjie Huang ([ljh@lanl.gov](mailto:ljh@lanl.gov))

**Keywords:** anisotropic media, borehole monitoring, enhanced geothermal systems, focal mechanism, hypocenter location, microearthquake, optimal design

## Highlights

- The paper presents a new methodology for optimal design of a 3D borehole seismic array for cost-effective microearthquake monitoring in anisotropic media.
- The method uses the relationships between seismic receiver distributions and standard deviation errors of microearthquake hypocenter locations and focal mechanisms.
- Our result demonstrates that microearthquake hypocenter locations and focal mechanisms can be reasonably well reconstructed for the EGS Collab Experiment I using three seismic receivers in each of six monitoring wells.

## ABSTRACT

Multiple U.S. national laboratories, universities and industrial collaborators are conducting collaborative research under the EGS Collab project supported by the U.S. Department of

---

<sup>1</sup> J. Ajo-Franklin, S.J. Bauer, T. Baumgartner, K. Beckers, D. Blankenship, A. Bonneville, L. Boyd, S.T. Brown, J.A. Burghardt, T. Chen, Y. Chen, K. Condon, P.J. Cook, P.F. Dobson, T. Doe, C.A. Doughty, D. Elsworth, J. Feldman, A. Foris, L.P. Frash, Z. Frone, P. Fu, K. Gao, A. Ghassemi, H. Gudmundsdottir, Y. Guglielmi, G. Guthrie, B. Haimson, A. Hawkins, J. Heise, C.G. Herrick, M. Horn, R.N. Horne, J. Horner, M. Hu, H. Huang, L. Huang, K. Im, M. Ingraham, T.C. Johnson, B. Johnston, S. Karra, K. Kim, D.K. King, T. Kneafsey, H. Knox, J. Knox, D. Kumar, K. Kutun, M. Lee, K. Li, R. Lopez, M. Maceira, N. Makedonska, C. Marone, E. Mattson, M.W. McClure, J. McLennan, T. McLing, R.J. Mellors, E. Metcalfe, J. Miskimins, J.P. Morris, S. Nakagawa, G. Neupane, G. Newman, A. Nieto, C.M. Oldenburg, W. Pan, R. Pawar, P. Petrov, B. Pietzyk, R. Podgorney, Y. Polsky, S. Porse, S. Richard, B.Q. Roberts, M. Robertson, W. Roggenthen, J. Rutqvist, D. Rynders, H. Santos-Villalobos, M. Schoenball, P. Schwering, V. Sesetty, A. Singh, M.M. Smith, H. Sone, C.E. Strickland, J. Su, C. Ulrich, N. Uzunlar, A. Vachaparampil, C.A. Valladao, W. Vandermeer, G. Vandine, D. Vardiman, V.R. Vermeul, J.L. Wagoner, H.F. Wang, J. Weers, J. White, M.D. White, P. Winterfeld, T. Wood, H. Wu, Y.S. Wu, Y. Wu, Y. Zhang, Y.Q. Zhang, J. Zhou, Q. Zhou, M.D. Zoback

Energy, to understand the fracture creation and imaging during fracturing in enhanced geothermal systems. Microearthquake hypocenter locations and focal mechanisms are used to monitor hydraulic fracturing growth and characterization at the EGS Collab experimental site at the Sanford Underground Research Facility using seismic receivers in multiple monitoring wells. We develop a methodology for optimal design a 3D borehole seismic array for cost-effective seismic monitoring in anisotropic media using not only the relationship between receiver distributions and standard deviation errors of microearthquake hypocenter locations, but also that between receiver distributions and focal-mechanism inversion errors. Our results indicate that microearthquake hypocenter locations and focal mechanisms can be reasonably well reconstructed for the EGS Collab Experiment I using six monitoring wells, including four fracture-parallel monitoring wells and two orthogonal wells. Eight seismic receivers evenly distributed in four parallel monitoring wells or twelve receivers in all six monitoring wells are required for hypocenter location, and twelve receivers evenly distributed in six wells or sixteen receivers in four wells are needed for focal-mechanism inversion.

## 1. INTRODUCTION

Enhanced geothermal systems (EGS) generate geothermal electricity without the need for natural convective hydrothermal resources. When natural cracks and pores do not achieve economic flow rates, stimulation could be used in EGS to create fractures and enhance the permeability. The original EGS concept was stimulation in hot dry rock originated at Los Alamos National Laboratory (Brown, 2009; Brown et al., 2012; Gallup, 2009; Olasolo et al., 2016). EGS offer tremendous potential as a renewable energy resource supporting the energy security of the United States. With a reasonable investment in R&D, EGS could provide 100 GWe or more of cost-competitive generating capacity in the next 50 years (Tester et al., 2006).

EGS development requires to accurately predict flow rates and temperatures in production wells. Complex heterogeneous fracture pathways can result in channeling, short-circuiting and premature thermal breakthrough, leading to complicated flow rate and temperature prediction. Multiple U.S. national laboratories, universities and industrial collaborators are conducting collaborative research under the EGS Collab project (Kneafsey et al., 2018b) supported by the U.S. Department of Energy's Geothermal Technologies Office (GTO), to understand the fracture

creation and imaging during fracturing in enhanced geothermal systems. The project is to address critical and fundamental barriers to EGS advancement using field stimulations at intermediate scale ( $\sim 10 - 20$  m). The project provides the opportunities for reservoir model prediction and validation, in coordination with in depth analysis of geophysical and other fracture characterization data, with an ultimate goal of understanding the basic relationship among stress, seismicity and permeability enhancement (Dobson et al., 2017; Kneafsey et al., 2018a; Kneafsey et al., 2018b). These experiments provide an opportunity of testing tools, codes, and concepts that could later be used for the EGS development at the Frontier Observatory for Research in Geothermal Energy (FORGE) site (Moore et al., 2018) and other enhanced geothermal systems. The FORGE is a dedicated site established by the U.S. Department of Energy GTO for scientists and engineers to develop, test, and accelerate breakthroughs in EGS technologies and techniques under the field EGS reservoir scale.

The EGS Collab project conducts field experiments at the Sanford Underground Research Facility (SURF) site located in Lead, South Dakota, at the former site of the Homestake Gold Mine (Figure 1). SURF is the host to a number of world-class physics experiments related to neutrino and dark matter, and geoscience research (Lesko, 2012; Mandic et al., 2018). As a mined underground research laboratory, SURF offers a number of advantages to promote the EGS Collab research, such as collecting high-quality and high-resolution geophysical and other fracture characterization and fluid flow data in a 3D borehole monitoring system. The experiment is within a drift located approximately 1.5 km beneath the surface. Seismic observation at depth can reduce human-made noise and seismic wave attenuation and scattering caused by the weathered and heterogeneous near-surface layers. Potential high signal-to-noise ratios (SNRs) of MEQ data and an optimally designed 3D borehole seismic array provide an unprecedented opportunity to reliably monitor and characterize fracture growth and unravel the physics of induced seismicity.

Figure 2 is a schematic illustration of the injection (in green) and production (in red) wells and six monitoring boreholes (in yellow) used during the Experiment I of stimulations in the EGS Collab project. The plan was to create fractures (blue circles in Figure 2) with the diameters of approximately 10 m. The six monitoring wells include four wells (PST, PSB, PDT and PBT in

Figure 2) parallel to, and two wells (OT, OB in Figure 2) orthogonal to the two potential fractures. The black spheres in Figure 2 are seismic receivers within those monitoring wells.

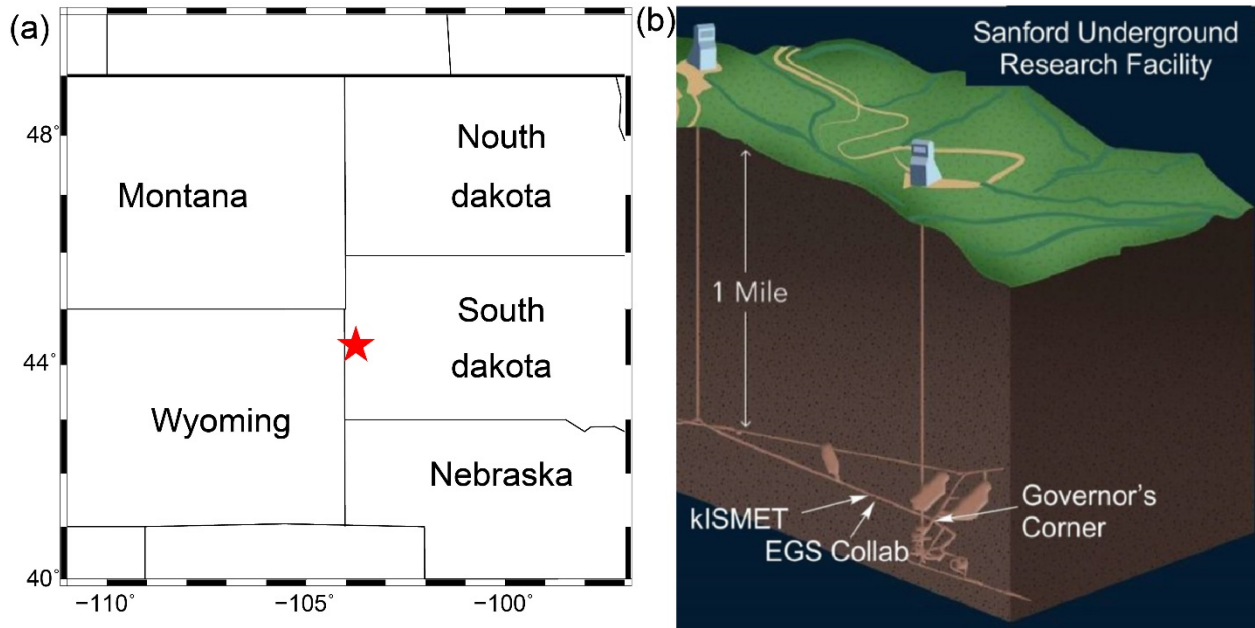


Figure 1: Geographic location (a) and schematic view (b) (Courtesy of Kneafsey et al., 2018b) of the Sanford Underground Research Facility. Red star represents SURF location in South Dakota.

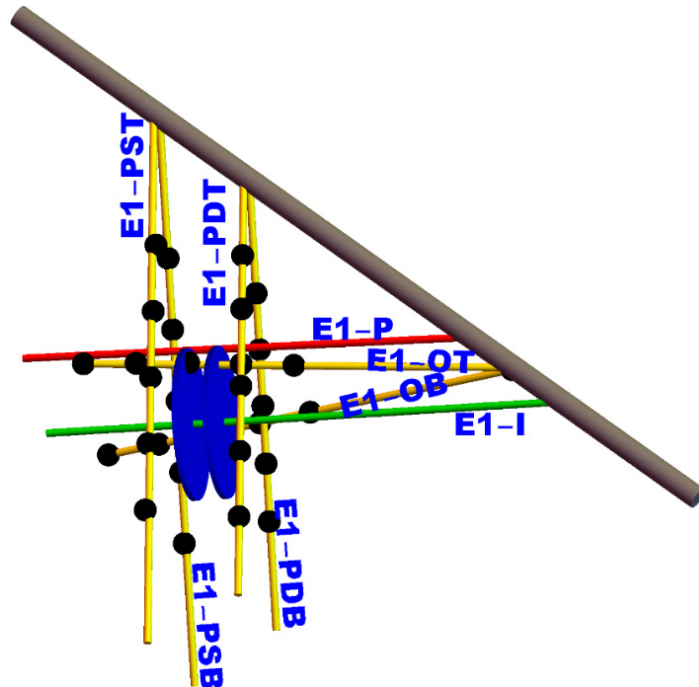


Figure 2: Schematic illustration of monitoring wells at SURF for the EGS Collab Experiment I. The monitoring wells (E1-PST, PSB, PDT, PDB, OT and OB) drilled from the drift (gray cylinder) are in

yellow. The injection well (E1-I) is green, and the production well (E1-P) is red. The circular regions in blue are the fractures to be created by hydraulic stimulations. The seismic receivers (black spheres) are distributed within the monitoring wells in yellow to monitor induced MEQs evenly distributed within the created fractures in the blue circular regions.

Microearthquake (MEQ) hypocenter location has been a ubiquitous tool for monitoring fracture growth and geomechanical deformation (Maxwell, 2014). The inversion accuracy strongly depends on the distribution of seismic receivers. Most previous studies on optimal designs of monitoring networks concentrated on surface monitoring networks and on monitoring natural earthquake location (Douglas, 1967; Havskov et al., 1992; Kijko, 1977a, 1977b; Rabinowitz and Steinberg, 1990; Yamada et al., 2011). Kijko (1977a; 1977b) presented an algorithm to minimize the ellipsoid volume of earthquake location errors and increase the earthquake location accuracy. Havskov et al. (1992) designed a seismic network to increase both the quantity and quality of real-time earthquake location from northern Norway. Yamada et al. (2011) used Monte-Carlo Markov chain algorithms to generate random network geometries and provide the design of future lunar seismic networks to retrieve the locations of moonquakes and impacts and lunar interior structures. Recently, Chen and Huang (2018) presented a synthetic study for optimal design of microseismic network for the Kimberlina CO<sub>2</sub> storage demonstration site. They designed a surface monitoring network based on minimizing only errors of microseismic hypocenter locations. The aforementioned methods used hypocenter location errors for the optimal seismic network design.

Rather than using surface seismic stations as the previous studies, the EGS Collab project employs a 3D borehole system for monitoring fracture creation and growth during stimulations. Besides MEQ hypocenter location, MEQ focal mechanism can further characterize fracture growth and MEQ event, such as: (1) Is each fault plane consistent with the whole fracture? (2) What is the stress status? (3) Do the MEQs have non-double-couple (NDC) components? (4) Can we use NDC components to distinguish crack opening and rupture in pre-existing fractures? Monitoring near the stimulation zones using the 3D borehole arrays have potential to address the above scientific problems.

In this paper, we develop a methodology for optimal design a 3D borehole seismic array for cost-effective seismic monitoring in anisotropic media using not only the relationship between receiver distributions and standard deviation errors of microearthquake hypocenter locations, but

also that between receiver distributions and focal-mechanism inversion errors. Our results indicate that microearthquake hypocenter locations and focal mechanisms can be reasonably well reconstructed for the EGS Collab Experiment I using six monitoring wells, including four fracture-parallel monitoring wells and two orthogonal wells. Eight seismic receivers evenly distributed in four parallel monitoring wells or twelve receivers in all six monitoring wells are required for hypocenter location, and twelve receivers evenly distributed in six wells or sixteen receivers in four wells are needed for focal-mechanism inversion.

## **2. DESIGN OF OPTIMAL SEISMIC NETWORK FOR MEQ EVENT-LOCATION MONITORING**

We develop a method to examine the hypocenter-location uncertainty for an MEQ event and seismic receiver distribution (Figure 3). The method first computes P- and S-wave travel times for a synthetic event to receivers, and then inverts hypocenter location for the synthetic event. The hypocenter-location uncertainty is defined as the standard deviation error of the event hypocenters.

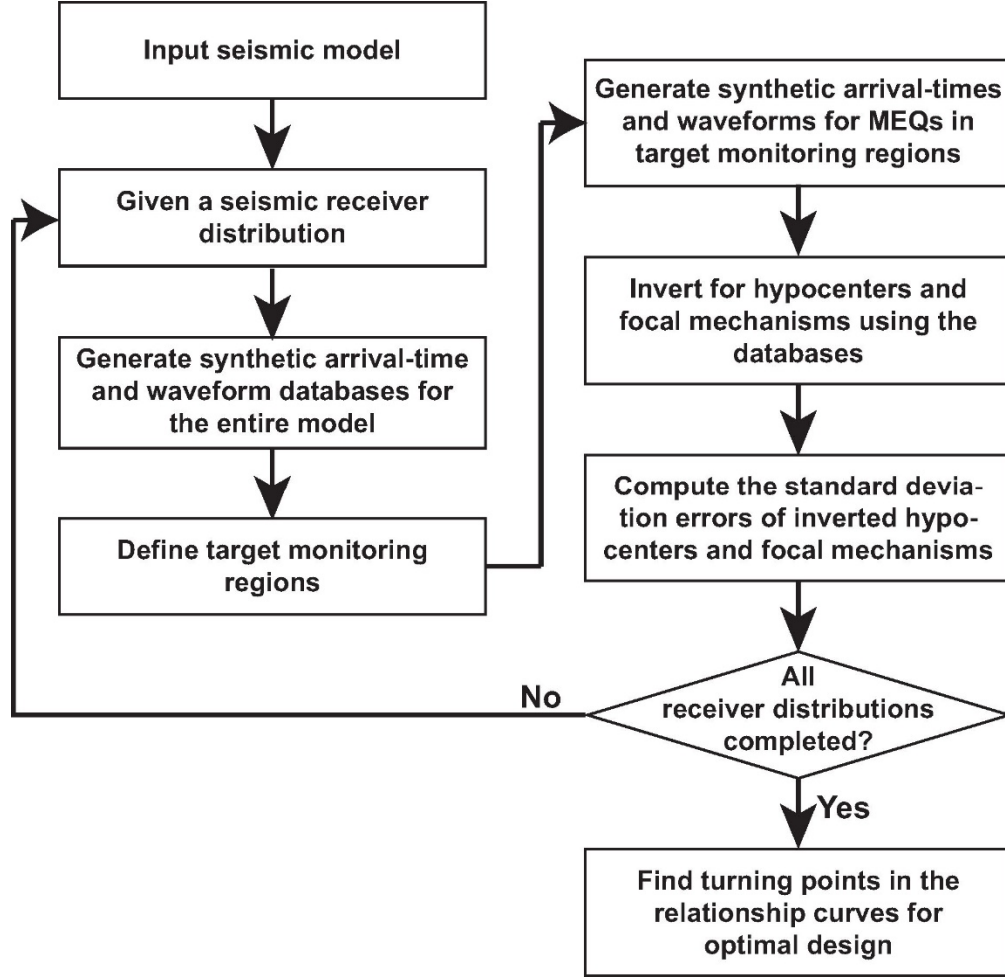


Figure 3: Flow-chart of our optimal design of a cost-effective monitoring network for MEQ hypocenter location and focal-mechanism inversion.

We develop an analytical method to calculate travel-time arrivals in homogeneous and anisotropic medium. For the vertical transverse isotropic (VTI) medium, we set the P-wave velocities along the fast and slow axes to be 6.5 km/s and 4.8 km/s, the S-wave velocities along the fast and slow axes to be 4.3 km/s and 3.3 km/s, and the density to be  $2.85 \times 10^3 \text{ kg/m}^3$ . The anisotropic model is built based on laboratory measurements of core samples from SURF (Huang et al., 2017). We calculate the stiffness matrix  $C_{ij}$  in the VTI medium as follows:

$$C = \begin{bmatrix} 120.4125 & 58.3395 & -29.1698 & 0 & 0 & 0 \\ & 120.4125 & -29.1698 & 0 & 0 & 0 \\ & & 65.664 & 0 & 0 & 0 \\ & & & 52.6965 & 0 & 0 \\ & & & & 52.6965 & 0 \\ & & & & & 31.0365 \end{bmatrix}.$$



We then adopt the Kelvin-Christoffel equation to estimate the slowness of the P and S waves in the specific direction (Carcione, 2007). The slowness can be used to obtain the P- and S-wave arrival times for any locations in this homogeneous, anisotropic medium.

We perform a non-linear inversion to obtain MEQ locations using P- and S-wave travel times. The inversion method adopts a simulated heat-annealing algorithm (Chen et al., 2014) to search for the best hypocenter location for a given event. The method minimizes the least-squares misfits between the predicted and observed P- and S-wave arrival times.

We use 162 MEQs evenly distributed within fracture planes shown in blue in Figure 2. The distance between MEQs along each axis of the Cartesian coordinate is 2 m. We study two scenario of seismic-receiver distributions, including four parallel wells and all six wells drilled for the project. The seismic receivers are evenly distributed in the range of 35 m within the wells and around the center of the fractures (Figure 2). For one geophone per well, the geophone is deployed at the middle of the well. For more geophones per well, two geophones are located at the both ends of the well and other geophones are evenly distributed in between. We study the relationships between MEQ hypocenter uncertainty and seismic receiver distributions for the EGS Collab Experiment I (Figure 4). Figure 4a exhibits the relationships between standard deviation errors of MEQ hypocenter locations and the total numbers of receivers evenly distributed within the four parallel (red curves) and all six monitoring wells (blue dashed curves), respectively. Generally, MEQ event location errors using four wells and six wells converges to almost the same level of errors when the total number of geophones is equal to and greater than 12. The results in Figure 4 indicate that eight receivers are required in four wells, while twelve receivers are needed in six wells to reach a reasonably small hypocenter uncertainty using noise-free travel-time picks. That is, two receivers in each well are needed for event hypocenter locations.

Figure 4b exhibits the same inversion but using noisy travel-time picks, which have a Gaussian distribution with a standard deviation of  $5 \times 10^{-5}$  seconds. The travel-time perturbation may be caused by P- and S-wave arrival time picks and an inaccurate velocity model used. Twelve receivers are required in either four or six wells. The uncertainty further decreases slightly as the number of receiver increases, because increasing the number of receivers statistically reduces the

effect from random noise of travel-time picks. The result demonstrates that the combination of parallel and orthogonal wells does not help for MEQ event location.

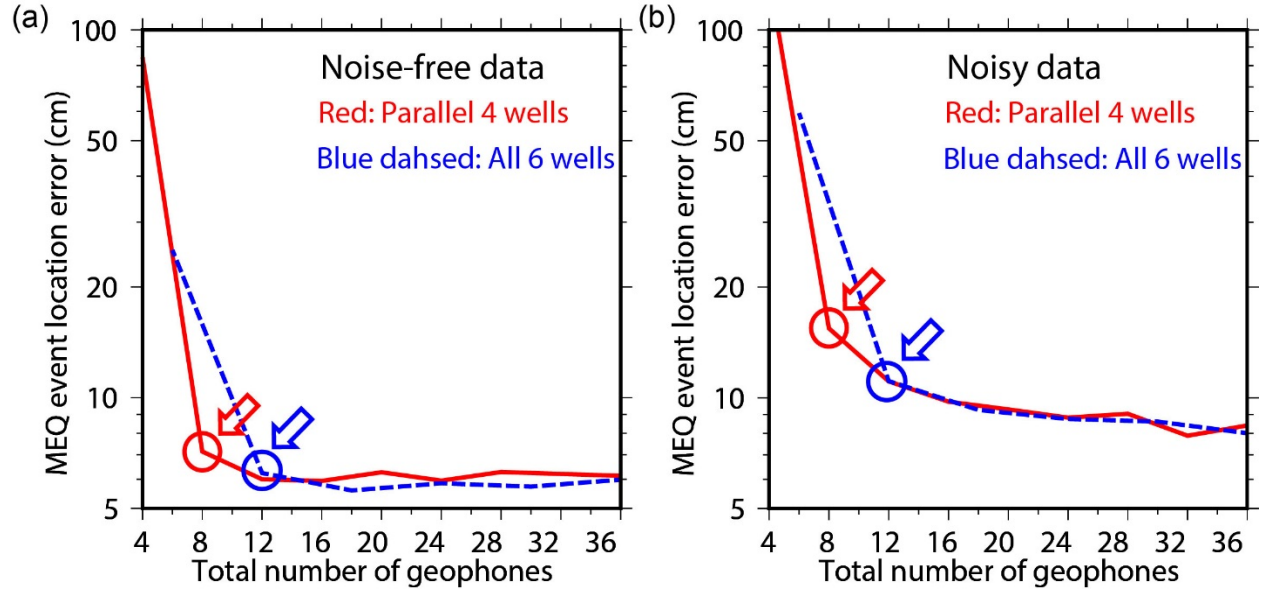


Figure 4: Standard deviation errors of MEQ event locations vs. the total numbers of seismic receivers evenly distributed within four parallel (red curves) and all six (blue dashed curves) monitoring wells as shown in Figure 2, for (a) noise-free travel-time picks and (b) noisy travel-time picks. The colored circles and arrows highlight turning points of the curves, representing optimal number of seismic receivers.

### 3. DESIGN OF OPTIMAL SEISMIC NETWORK FOR MEQ FOCAL-MECHANISM INVERSION

We develop a focal-mechanism inversion method to study MEQ focal-mechanism inversion uncertainty for an MEQ source and seismic receiver configuration (Figure 3). Full focal mechanism can be decomposed as strike, dip, rake for the double-couple component of focal mechanisms, ISO (isotropic component) and compensated linear vector dipole (CLVD) for the non-double-couple component of focal mechanism, and seismic moment. Double-couple component would exhibit the fault geometry, while non-double-couple component can reveal crack opening. Here, we adopt seven parameters to represent each event, including strike, dip, rake, ISO, CLVD, and source duration and moment.

We calculate Green's functions using an anisotropic finite-difference waveform modeling method (Gao and Huang, 2017), based on the same velocity/stiffness model adopted in Section 2. The synthetics are the combination of the Green's functions based on the focal mechanism,

and then convolved with source duration and moment. We generate synthetic data using given source parameters. We invert for the seven source parameters using the simulated heat-annealing algorithm (Chen et al., 2014) to minimize the misfit between the synthetic data and the predicted synthetics. The objective function (misfit) is  $\sum_{n=1}^N \sum_{j=1}^J \|d_j^n - s_j^n\|_2$ , where  $j$  is the channel number and  $n$  is the event number,  $d_j^n$  is a seismic trace normalized to the maximum absolute amplitude to each channel, and  $s_j^n$  is the normalized synthetic trace. We search a half parameter space for a strike of  $0^\circ - 360^\circ$ , dip of  $0^\circ - 90^\circ$  and rake of  $-90^\circ - 90^\circ$ . The search ranges of the ISO and CLVD components are -1 to 1 and -0.5 to 0.5, respectively.

We study the relationships between MEQ focal-mechanism standard deviation errors and seismic receiver distribution configurations within four parallel and all six monitoring wells for the EGS Collab Experiment I (Figure 2). The configuration of source and receiver distributions is the same as that in Section 2. To simplify the comparison, we define the MEQ double-couple error as the average of strike, dip and slip standard deviation errors, MEQ non-double-couple error as the average of ISO and CLVD standard deviation errors, and MEQ focal-mechanism error as the average of strike/360, dip/90, rake/360, ISO, and CLVD/0.5.

Figure 5a displays the relationships between MEQ focal-mechanism errors and the total numbers of receivers evenly distributed within four parallel and all six monitoring wells, respectively. Twelve receivers in six wells (blue dashed curve in Figure 5a) or sixteen receivers in four wells (red curve in **Error! Reference source not found.**a) are required for reliable focal-mechanism inversion.

In Figure 5b, we show the inversion results for synthetic data with 20% white noise. Eighteen receivers in six wells or twenty in four wells are needed for noisy data. Figure 5 indicates that using all six wells improves capability of recovering focal mechanism when the receiver number is less than sixteen. However, the two scenarios work equally well when the receiver number is more than sixteen. We note that standard deviation errors still decrease as the receiver number increase. For cost-effective monitoring, we suggest that using twelve receivers evenly distributed in all six wells is the optimal design.

We also plot the relationships between double-couple component of MEQ focal-mechanism errors and the total number of receivers in Figure 6, and that between non-double-couple component errors and the total number of receivers in Figure 7. We obtain similar conclusions as in Figure 5. Our optimal network can acquire double-couple error as low as  $0.4^\circ$  and non-double-couple error as low as 0.005.

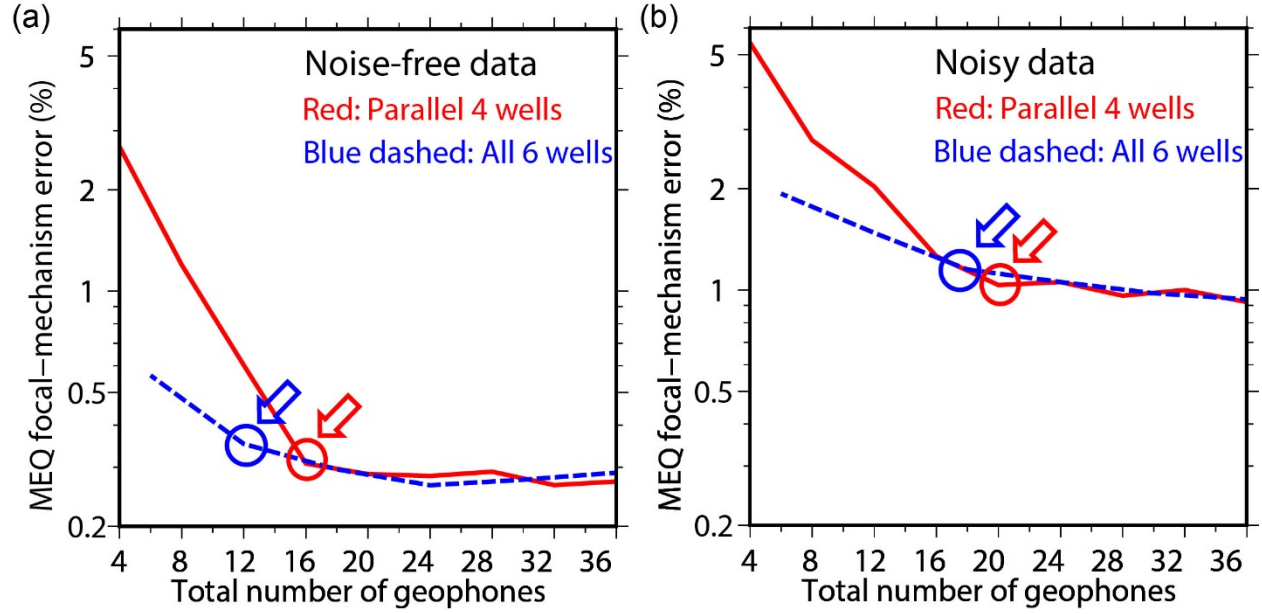


Figure 5: Standard deviation errors of MEQ focal mechanisms vs. the total numbers of seismic receivers evenly distributed within four parallel (red curves) and all six (blue dashed curves) monitoring wells as shown in Figure 2, for (a) noise-free synthetic data and (b) noisy synthetic data.

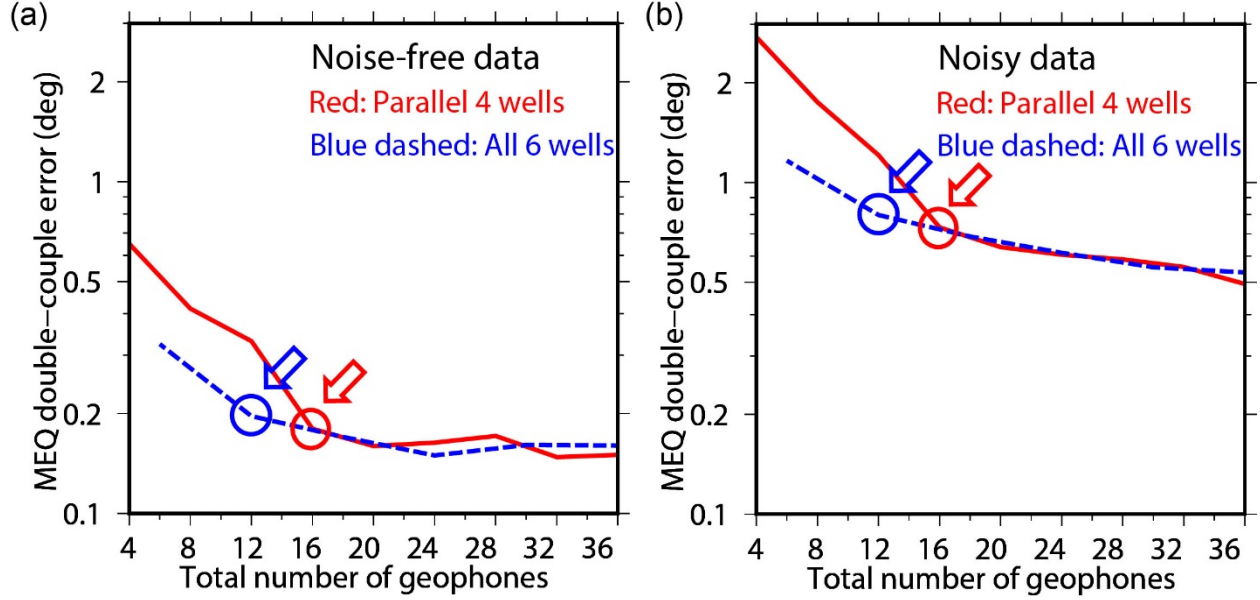


Figure 6: Standard deviation errors of double-couple components of MEQ focal mechanisms vs. the total numbers of seismic receivers evenly distributed within four parallel (red curves) and all six (blue dashed curves) monitoring wells as shown in Figure 2, for (a) noise-free synthetic data and (b) noisy synthetic data.

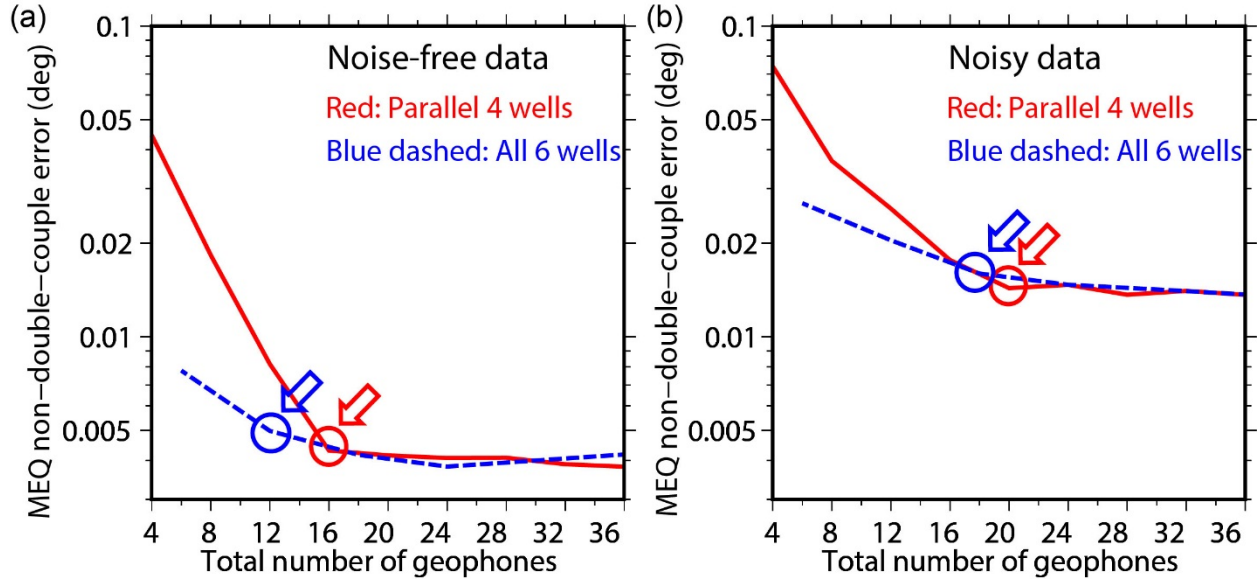


Figure 7: Standard deviation errors of non-double-couple components of MEQ focal mechanisms vs. the total numbers of seismic receivers evenly distributed within four parallel (red curves) and all six (blue dashed curves) monitoring wells as shown in Figure 2, for (a) noise-free synthetic data and (b) noisy synthetic data.

#### 4. CONCLUSIONS

We have developed a methodology for optimal design of a 3D borehole seismic array for microearthquake hypocenter location and focal mechanism inversion in anisotropic media for the

EGS Collab Experiment I at the Sanford Underground Research Facilities in South Dakota, USA. In the method, we minimize the misfits between seismic arrive-times and waveforms for MEQs in target monitoring regions and those in a pre-generated database for the entire model, and use a simulated heat-annealing algorithm to invert for hypocenter locations and focal mechanisms. We study standard deviation errors of hypocenter locations and focal mechanisms, and use the relationships between standard deviation errors and seismic receiver distributions for optimal design of MEQ monitoring arrays.

Our numerical study demonstrates that microearthquake hypocenter locations and focal mechanisms can be reasonably well reconstructed for the EGS Collab Experiment I using six monitoring wells, including four fracture-parallel monitoring wells and two orthogonal wells. Eight seismic receivers evenly distributed in four parallel monitoring wells or twelve receivers in all six monitoring wells are required for hypocenter location, and sixteen receivers evenly distributed in four wells or twelve receivers in all six wells are needed for focal-mechanism inversion. More receivers would help reduce the inversion uncertainty caused by strong noise.

Our method is applicable to other optimal designs of either surface and/or borehole seismic monitoring networks for other studies, such as microseismic monitoring of hydrogeothermal production and enhanced geothermal systems. The method generates a number of synthetic microseismic events within target monitoring regions, inverts their locations and focal mechanisms using different seismic receiver distributions, and calculates standard deviation errors of event locations and focal mechanisms. The optimal design can then be derived from the standard deviation error curves.

## ACKNOWLEDGMENTS

This material was based upon work supported by the U.S. Department of Energy, Office of Energy Efficiency and Renewable Energy (EERE), Office of Technology Development, Geothermal Technologies Office, under Award Number DE-AC52-06NA25396 to Los Alamos National Laboratory (LANL). We thank Editor Christopher Bromley and two anonymous reviewers for their constructive comments to improve the paper. The United States Government retains, and the publisher, by accepting the article for publication, acknowledges that the United

States Government retains a non-exclusive, paid-up, irrevocable, world-wide license to publish or reproduce the published form of this manuscript, or allow others to do so, for United States Government purposes. The computation was performed using super-computers of LANL's Institutional Computing Program.

## REFERENCES

Brown, D.W., 2009. Hot dry rock geothermal energy: important lessons from Fenton Hill, Proceedings of the Thirty-Fourth Workshop on Geothermal Reservoir Engineering, Stanford University, California.

Brown, D.W., Duchane, D.V., Heiken, G., Hriscu, V.T., 2012. Mining the earth's heat: hot dry rock geothermal energy. Springer Science & Business Media.

Carcione, J.M., 2007. Wave fields in real media: Wave propagation in anisotropic, anelastic, porous and electromagnetic media. Elsevier.

Chen, T., Huang, L., 2018. Optimal design of microseismic monitoring network: Synthetic study for the Kimberlina CO<sub>2</sub> storage demonstration site. International Journal of Green House Gas Control, under review

Chen, Y., Wen, L., Ji, C., 2014. A cascading failure during the 24 May 2013 great Okhotsk deep earthquake. Journal of Geophysical Research: Solid Earth 119, 3035-3049.

Dobson, P., Kneafsey, T.J., Blankenship, D., Valladao, C., Morris, J., Knox, H., Schwering, P., White, M., Doe, T., Roggenthen, W., Team, t.E.C., 2017. An introduction to the EGS Collab project. GRC Transation, 41, 837-849.

Douglas, A., 1967. Joint Epicentre Determination. Nature 215, 47.

Gallup, D.L., 2009. Production engineering in geothermal technology: A review. Geothermics 38, 326-334.

Gao, K., Huang, L., 2017. An improved rotated staggered-grid finite-difference method with fourth-order temporal accuracy for elastic-wave modeling in anisotropic media. Journal of Computational Physics 350, 361-386.

Havskov, J., Kvamme, L., Hansen, R., Bungum, H., Lindholm, C., 1992. The northern Norway seismic network: Design, operation, and results. Bulletin of the Seismological Society of America 82, 481-496.

Huang, L., Chen, Y., Gao, K., Fu, P., Morris, J., Ajo-Franklin, J., Nakagawa, S., and EGS Collab Team, 2017. Numerical modeling of seismic and displacement-based monitoring for the EGS Collab Project. GRC Transaction, 41, 893-909.

- 305 Kijko, A., 1977a. An algorithm for the optimum distribution of a regional seismic network—I.  
306 pure and applied geophysics 115, 999-1009.
- 307 Kijko, A., 1977b. An algorithm for the optimum distribution of a regional seismic network—II.  
308 An analysis of the accuracy of location of local earthquakes depending on the number of  
309 seismic stations. pure and applied geophysics 115, 1011-1021.
- 310 Kneafsey, T., Blankenship, D., Dobson, P., Knox, H., Johnson, T., Ajo-Franklin, J., Schwering,  
311 P., Morris, J., White, M., Podgorney, R., Roggenthen, W., Doe, T., Mattson, E., Valladao,  
312 C., Team, t.E.C., 2018a. EGS Collab Project Experiment I Overview and Progress. GRC  
313 Transation, 42, 2018.
- 314 Kneafsey, T.J., Dobson, P., Blankenship, D., Morris, J., Knox, H., Schwering, P., White, M.,  
315 Doe, T., Roggenthen, W., Mattson, E., Team, t.E.C., 2018b. An Overview of the EGS  
316 Collab Project: Field Validation of Coupled Process Modeling of Fracturing and Fluid Flow  
317 at the Sanford Underground Research Facility, Lead, SD, Proceedings of 43rd Workshop on  
318 Geothermal Reservoir Engineering, Stanford University, California.
- 319 Lesko, K.T., 2012. The Sanford Underground Research Facility at Homestake. European  
320 Physical Journal Plus 127.
- 321 Mandic, V., Tsai, V.C., Pavlis, G.L., Prestegard, T., Bowden, D.C., Meyers, P., Caton, R., 2018.  
322 A 3D Broadband Seismometer Array Experiment at the Homestake Mine. Seismological  
323 Research Letters 89, 2420-2429.
- 324 Maxwell, S., 2014. Microseismic imaging of hydraulic fracturing: Improved engineering of  
325 unconventional shale reservoirs. Society of Exploration Geophysicists.
- 326 Moore, J., McLennan, J., Allis, R., Pankow, K., Simmons, S., Podgorney, R., Wannamaker, P.,  
327 Rickard, W., 2018. The Utah Frontier Observatory for Geothermal Research (FORGE):  
328 Results of Recent Drilling and Geoscientific Survey, Geothermal Resources Council 42nd  
329 Annual Meeting-Geothermal Energy, GRC 2018.
- 330 Olasolo, P., Juarez, M.C., Morales, M.P., D'Amico, S., Liarte, I.A., 2016. Enhanced geothermal  
331 systems (EGS): A review. Renew. Sust. Energ. Rev. 56, 133-144.
- 332 Rabinowitz, N., Steinberg, D.M., 1990. Optimal configuration of a seismographic network: a  
333 statistical approach. Bulletin of the Seismological Society of America 80, 187-196.
- 334 Tester, J.W., Anderson, B.J., Batchelor, A.S., Blackwell, D.D., DiPippo, R., Drake, E., Garnish,  
335 J., Livesay, B., Moore, M.C., Nichols, K., 2006. The future of geothermal energy: Impact of  
336 enhanced geothermal systems (EGS) on the United States in the 21st century. Massachusetts  
337 Institute of Technology 209.



338 Yamada, R., Garcia, R.F., Lognonné, P., Le Feuvre, M., Calvet, M., Gagnepain-Beyneix, J.,  
339 2011. Optimisation of seismic network design: application to a geophysical international  
340 lunar network. Planetary and Space Science 59, 343-354.